Spectral and optical characteristics of spheroidal quantum dots

2012 J. Phys.: Conf. Ser. 393 012011

(http://iopscience.iop.org/1742-6596/393/1/012011)

Journal of Physics: Conference Series **393** (2012) 012011 doi:10.1088/1742-6596/393/1/012011

Spectral and optical characteristics of spheroidal quantum dots

A A Gusev[1], O Chuluunbaatar[1], L L Hai[1], S I Vinitsky[1], E M Kazaryan [2], H A Sarkisyan [2] and V L Derbov [3]

[1] Joint Institute for Nuclear Research, Dubna, Russia
[2] Russian-Armenian (Slavonic) University, Yerevan, Armenia
[3] Saratov State University, Saratov, Russia

E-mail: gooseff@jinr.ru

Abstract. In the framework of effective mass approximation and in strong size quantization regime the absorption coefficients for ensembles of spheroidal quantum dots (SQDs) are analyzed using the eigenvalues and eigenfunctions, calculated by means of Kantorovich and adiabatic methods. The comparison of absorption coefficients for oblate and prolate SQDs with parabolic and non-parabolic dispersion laws reveals different behavior depending on the aspect ratio (ratio of minor to major semiaxis) and the external homogeneous electric fields. The possibility of verification of the considered models is discussed.

1. Introduction

Quantum dots (QDs) are considered to be promising as the elementary basis for the new generation of semiconductor devices [1]. The unique opportunity to perform the energy level control and flexible manipulation in QDs is due to the full quantization of charge carrier energy spectra in these systems. This allows design and manufacturing of artificial structures with prescribed quantum physical characteristics [2]. That is why the scope of QDs potential applications is very wide, from heterostructure lasers to nanomedicine and nanobiology. An impressive example of such application is represented by QD lasers possessing low threshold current and high efficiency [2].

The peculiarities of physical processes in QDs are caused by both their composition and geometry. Electronic, kinetic, optical and other properties of QDs have been investigated experimentally and theoretically in many papers [3]–[15]. Particularly, the optical absorption characteristics of QDs have been shown to be strongly correlated with their geometry, on one hand, and their physical–chemical properties, on the other hand. In one of the first publications on optical transitions in QD [16] the interband absorption of light was considered in the ensemble of weakly interacting spherical QDs implanted in a dielectric matrix. The dispersion of QD sizes was characterized in the framework of Lifshitz–Slezov theory [17]. It was shown that in the absence of size dispersion, due to the full quantization of charge carriers energy spectra in QD, the absorption coefficient behaves like a delta function, and the absorption threshold frequencies depend on the peculiarities of electron and hole energy spectra. When the QD size dispersion is taken into account, the averaging procedure yields the absorption profile having finite width and height.

Recently several reports concerning the experimental implementation of narrow-band InSb QDs have appeared [18, 19], in which the dispersion law for electrons and light holes is non-parabolic and described according to the double-band mirror Kane model [20, 21]. For non-interacting band of heavy holes the dispersion law is considered as quadratic. The investigation of optical absorption peculiarities in InSb QDs is an interesting problem, taking the electron transitions from light and heavy hole bands induced by the absorbed photon energy to the conduction band into account. Interband transitions in an ensemble of cylindrical or spherical InSb QDs were considered theoretically in dipole approximation with and without magnetic field, including excitonic effects, by means of perturbation and adiabatic methods [22]–[24]. The realization of ellipsoidal QDs were done recently and experiments are intensified just nowadays. Unfortunately, the experiments of growth of ellipsoidal QDs we are aware of, are about InAsSbP compounds the zone structure of which is investigated poorly.

Quantum dots with ellipsoidal geometry are difficult to describe analytically. Therefore, one has to use numerical description of electronic and optical properties of such systems [25]–[31]. It is clear that for the first stage of investigation it is reasonable to discuss one particle states (strong size quantization regime), as far as in that case the problem becomes relatively simple. The criteria of applicability of such approximation are conditioned by the correctness of the following inequalities: $d_{max} \ll a_B^e$ and $d_{max} \ll a_B^h$, where d_{max} is the biggest linear size of localization area of electron and hole with respect to the corresponded Bohr radius,$a_B^{e,h} = (\hbar^2\kappa)/(\mu_{e,h}e^2)$, in the effective mass approximation of the $\mathbf{k}\cdot\mathbf{p}$-theory. Here, κ is the dc permittivity, $\mu_{e(h)} = \beta_{e(h)}m_0$ is the effective mass of electron or hole, m_0 is the mass of electron. As known, a comparison of theory with experiment show, if a sample thickness in a direction of size quantization contains more then ten crystal layers, i.e. start from 30-40 angstrom, then one can use effective mass approximation [1]. It should be mention, that in paper [7] in the same approximation the authors discussed the absorption of light in ellipsoidal quantum dot with asymmetric parabolic confinement potential in the presence of magnetic field. The problem of optical absorption was discussed on the base of normal mode approach [8] and exact expressions for interband transition threshold frequencies were found.

The consideration of excitonic effects is possible to do in several steps. In the case of weak size quantization regime the main energy contribution of the system is defined by the Coulomb energy of electron-hole interaction, and the presence of size quantization it is possible to define by the influence of walls on the center of mass of exciton (see, for example, [16]). Thereby, in this case the relative motion can be separated from the motion of center of mass and the shift (displacement) of excitonic line is taking place at the expense of size quantization of the motion of exciton as a whole. In the case of intermediate size quantization when for the heavy hole the size quantization is not significant, but for the electron it is strong enough, it is necessary to apply adiabatic approximation, when the motion of the hole is described in an effective field of a fast moving electron. The solution of excitonic problems of QD with ellipsoidal geometry needs separate and detailed study [9, 10]. Therefore within the frameworks of this paper we would not discuss excitonic effects, as well as electron-electron and hole-hole interactions.

Earlier we elaborated calculation schemes, symbolic-numerical algorithms (SNAs) and programs for numerical solution of boundary-value problems (BVPs) in axially-symmetric models of quantum wells, quantum wires and QDs in external fields, using the effective mass approximation [30]–[41]. The programs were based on the generalized Kantorovich method and the adiabatic method, allowed calculation of both discrete and continuous spectra and provided the prescribed accuracy.

In the present paper we apply the developed approach to the analysis of spectral and optical characteristics of oblate and prolate spheroidal QDs in strong size quantization regime with parabolic and non-parabolic dispersion laws under the influence of homogeneous electric fields (HEFs), i.e., the quantum-confined Stark effect.

2. Statement of the problem

Let us consider in the effective mass approximation of the $\mathbf{k}\cdot\mathbf{p}$-theory spheroidal QDs in strong size quantization regime with possible influence of the uniform electric field $\mathbf{F} = (0, 0, F)$. Then the Schrödinger equation for the slow-varying envelope wave function $\tilde{\Psi}^i(\tilde{\mathbf{r}_i})$ of an electron ($i = e$) or a hole ($i = h$) reads as [10]:

$$\left\{\frac{1}{2\mu_i}\tilde{\hat{\mathbf{p}}}_i^{\,2} - q_i(\mathbf{F}\cdot\tilde{\mathbf{r}_i}) + \tilde{U}_{conf}(\tilde{\mathbf{r}_i}) - \tilde{E}^i\right\}\tilde{\Psi}^i(\tilde{\mathbf{r}_i}) = 0. \tag{1}$$

Here $\tilde{\mathbf{r}_i}$ is the radius-vector, $\tilde{\mathbf{r}_i} = (\tilde{x_i}, \tilde{y_i}, \tilde{z_i})$, $\tilde{\hat{\mathbf{p}}}_i = -i\hbar\nabla_{\tilde{\mathbf{r}_i}}$ is the momentum, $\tilde{E}^i$ is the energy of particles, $q_e = -e$ and $q_h = +e$ are the Coulomb charges of the electron and the hole, For the model under consideration, $\tilde{U}_{conf}(\tilde{\mathbf{r}})$ is the potential of a spherical or axially-symmetric well

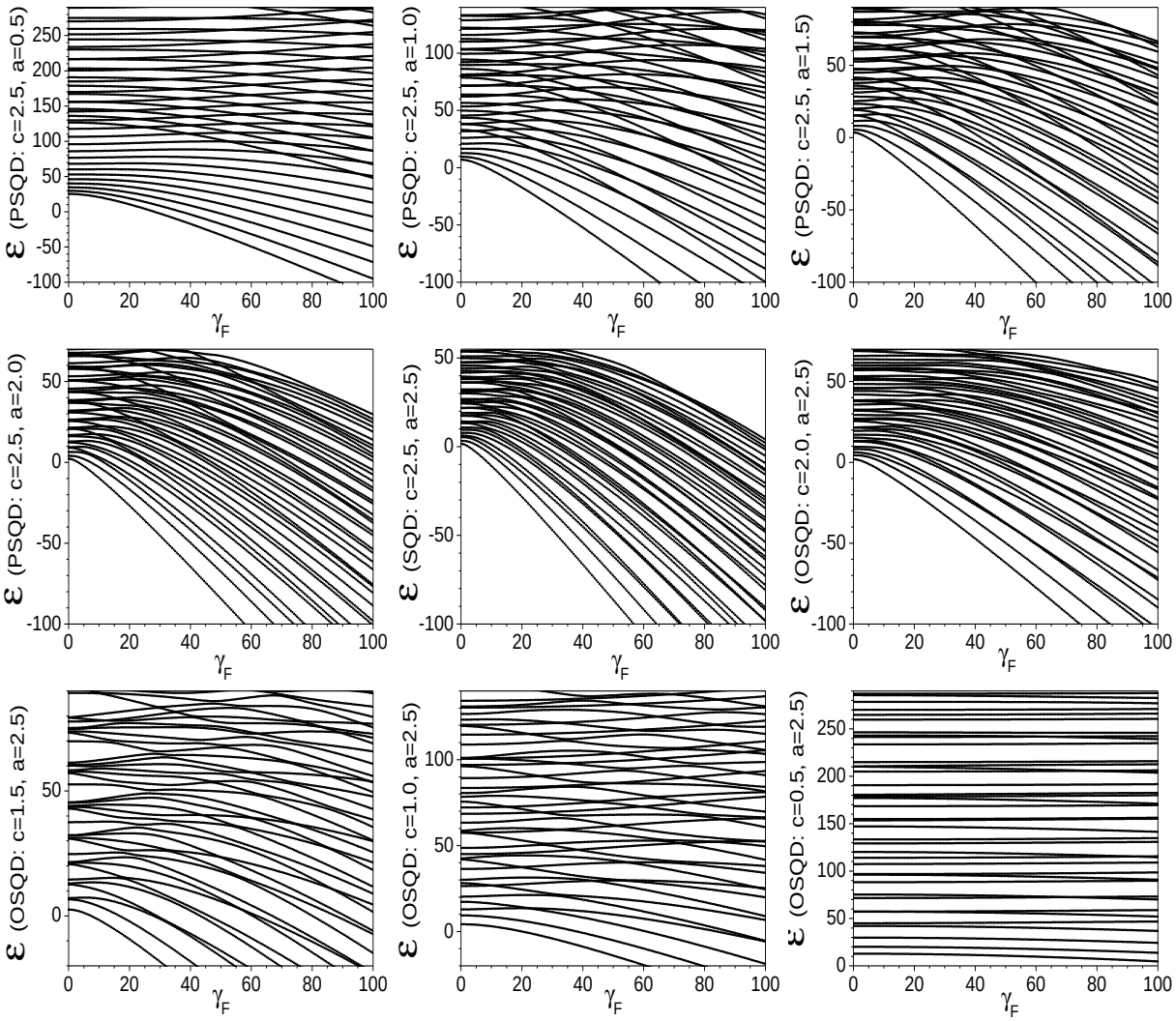

Figure 1. Dependence of energy eigenvalues $\mathcal{E}$ (in units of E_R^e) of the lower part of the spectrum of electronic states of QDs at $m = 0$ upon the electric field strength γ_F (in units of F_0^*): for spherical quantum dot (SQD) with radius $a = c = 2.5$, oblate and prolate spheroidal quantum dots (OSQD and PSQD) at different minor semiaxis (for OSQD $c = 0.5, 1, 1.5, 2$, $a = 2.5$, for PSQD $c = 2.5$, $a = 0.5, 1, 1.5, 2$).

$\tilde{U}_{conf}(\tilde{\mathbf{r}}_i) = \{0, S(\tilde{\mathbf{r}}_i) < 0; \tilde{U}_0, S(\tilde{\mathbf{r}}_i) \geq 0\}$, bounded by the surface $S(\tilde{\mathbf{r}}_\mathbf{i}) = 0$ with walls of infinite height (infinite potential barrier model, IPBM) or finite height $1 \ll \tilde{U}_0 < \infty$ (finite potential barrier model, FPBM). Here $S(\tilde{\mathbf{r}}_i)$ depends on the parameters $\tilde{a}$, $\tilde{c}$, which are semiaxes of a spheroidal QD, $S(\tilde{\mathbf{r}}_i) \equiv (\tilde{x}_i^2 + \tilde{y}_i^2)/\tilde{a}^2 + \tilde{z}_i^2/\tilde{c}^2 - 1$. The eigenvalues and eigenfunctions needed to evaluate the absorption coefficients (ACs) were calculated with prescribed accuracy by means of program packages ODPEVP and KANTBP [34, 35, 36]. For example, the energy eigenvalues $\mathcal{E} = 2E^e = \tilde{E}^e/E_R^e$ of the lower part of the electronic spectrum of the QDs at $m = 0$ versus the electric field strength $2\gamma_F = F/F_0^*$ (in the reduced atomic units [4]) for the IPBMs of spherical, oblate, and prolate spheroidal QDs with parabolic dispersion law at different values of minor semiaxis are shown in Fig. 1. Detailed explanation of these dependencies is given in the forthcoming paper [41]. The dependence of the IPBMs and FPBMs of spheroidal and dumbbell ODs on the minor semiaxis was studied in [30, 31].

3. Absorption coefficient for an ensemble of QDs

One can use differences in the energy spectra to verify the considered models of QDs by calculating the absorption coefficient $K(\tilde{\omega}^{ph}, \tilde{a}, \tilde{c},)$ of an ensemble of identical semiconductor QDs [16]. Since we do not discuss exciton effects in the present paper, the absorption coefficient may be approximately expressed as

$$\tilde{K}(\tilde{\omega}^{ph}, \tilde{a}, \tilde{c}, u) = \sum_{\nu,\nu'} \tilde{K}_{\nu,\nu'}(\tilde{\omega}^{ph}, \tilde{a}, \tilde{c}, u) = \tilde{A} \sum_{\nu,\nu'} \tilde{I}_{\nu,\nu'}(u) \delta(\hbar\tilde{\omega}^{ph} - \tilde{W}_{\nu\nu'}), \tag{2}$$

$$\tilde{I}_{\nu,\nu'}(u) = \left| \int \tilde{\Psi}_\nu^e(\tilde{\mathbf{r}}; \tilde{a}, \tilde{c}, F, \mu_e) \tilde{\Psi}_{\nu'}^h(\tilde{\mathbf{r}}; \tilde{a}, \tilde{c}, F, \mu_h) d^3\tilde{\mathbf{r}} \right|^2,$$

where $\tilde{A}$ is proportional to the square of the matrix element in the Bloch decomposition, $\tilde{\Psi}_\nu^e(u)$ and $\tilde{\Psi}_{\nu'}^h$ are the eigenfunctions of the electron (e) and the heavy hole (h), $\tilde{E}_\nu^e$ and $\tilde{E}_{\nu'}^h$ are the energy eigenvalues for the electron (e) and the heavy hole (h), depending on the semiaxis size $\tilde{c}, \tilde{a}$ for OSQD (or $\tilde{a}, \tilde{c}$ for PSQD) and the adiabatic set of quantum numbers $\nu = [n_{zo}, n_{\rho o}, m]$ and $\nu' = [n'_{zo}, n_{\rho o'}, m']$ ($\nu = [n_{\rho p}, n_{zp}, m]$ and $\nu' = [n'_{\rho p}, n'_{zp}, m']$), where $m' = -m$, $\tilde{E}_g$ is the band gap width in the bulk semiconductor, $\tilde{\omega}^{ph}$ is the incident light frequency, $\tilde{W}_{\nu\nu'} = \tilde{E}_g + \tilde{E}_\nu^e(\tilde{a}, \tilde{c}) + \tilde{E}_{\nu'}^h(\tilde{a}, \tilde{c})$ is the inter-band transition energy for which $\tilde{K}(\tilde{\omega}^{ph})$ has the maximal value. We rewrite the expression (2) in the terms of frequency shift of the incident light $\Delta\omega^{ph}/(2\pi) = (\hbar\tilde{\omega}^{ph} - \tilde{E}_g)/(2\pi\hbar)$ corresponding to the inter-band transition energy shift $\Delta\tilde{W}_{\nu\nu'} = \tilde{W}_{\nu\nu'} - \tilde{E}_g = \tilde{E}_\nu^e(\tilde{a}, \tilde{c}) + \tilde{E}_{\nu'}^h(\tilde{a}, \tilde{c})$ for which $\tilde{K}(\Delta\tilde{\omega}^{ph})$ has the maximal value, using dimensionless variables in reduced atomic units

$$\tilde{K}(\Delta\tilde{\omega}^{ph}, \tilde{a}, \tilde{c}) = \tilde{A}\tilde{E}_g^{-1} \sum_{\nu,\nu'} \tilde{I}_{\nu,\nu'}(u) \delta[f_{\nu,\nu'}(u)], \quad f_{\nu,\nu'}(u) = \lambda_1 - \frac{2E_\nu^e(a,c) + 2E_{\nu'}^h(a,c)(\mu_h/\mu_e)}{2E_g}, \tag{3}$$

Here the parameter u will be defined below, $\lambda_1 = (\hbar\tilde{\omega}^{ph} - \tilde{E}_g)/\tilde{E}_g$ is the energy of the optical interband transitions scaled to $\tilde{E}_g$, $2E_g = \tilde{E}_g/\tilde{E}_R^e$ is the dimensionless band gap width.

For GaAs the functions $f_{\nu,\nu'}^{h\to e}(u)$ describing the $(h \to e)$ interband transitions have the form

$$f_{\nu,\nu'}^{h\to e}(u) = \lambda_1 - (2E_g)^{-1}(2E_\nu^e(a,c) + 2E_{\nu'}^e(a,c)(\mu_e/\mu_h)), \tag{4}$$

where $\mu_e = 0.067m_0$ and $\mu_h = 0.558m_0$ are the masses of electron and holes, respectively, $\tilde{E}_g = 1430$meV is the band gap width and $\kappa = 13.18$ is the dc permittivity and $E_R^e = e^2/(2\kappa a_B^e) = 5.275$ meV, $a_B^e = \hbar^2\kappa/(\mu_e e^2) = 104$Å, $E_R^h = e^2/(2\kappa a_B^h) = 49$ meV, $a_B^h = \hbar^2\kappa/(\mu_h e^2) = 15$Å and $F_0^* = E_R^e/(ea_B^e) = e/(2\kappa(a_B^e)^2) = 5.04$kV/cm.

For InSb the dispersion law for heavy holes (hh) is parabolic while for electrons (e) and light holes (lh) it is non-parabolic and may be described by the Kane model [20, 21, 24]. The energy values in our notation are:

$$2\tilde{E}^{hh}_{\nu}(InSb) = 2\tilde{E}^{h}_{\nu'}(\tilde{a},\tilde{c}), \tag{5}$$

$$2\tilde{E}^{e}_{\nu}(InSb) = 2\tilde{E}^{lh}_{\nu}(InSb) = -\tilde{E}_g/2 + \sqrt{\tilde{E}_g^2/4 + \tilde{E}_g(2\tilde{E}^{e}_{\nu}(\tilde{a},\tilde{c}))}. \tag{6}$$

As follows from Eqs. (5) and (8), to determine the energy spectrum and the wave function of the light hole and the electron one should solve the Klein-Gordon equation [42, 43], while for heavy hole the Schrödinger equation is applicable. The functions $f^{hh\to e}_{\nu,\nu'}(u)$ and $f^{hh\to e}_{\nu,\nu'}(u)$ describing the $(hh \to e)$ and the $(lh \to e)$ interband transitions have the forms

$$f^{hh\to e}_{\nu,\nu'}(u) = \lambda_1 - (1/2 + \sqrt{1/4 + (2E^{e}_{\nu}(a,c)/(2E_g))} + (2E_g)^{-1}2E^{e}_{\nu'}(a,c)(\mu_e/\mu_h)), \tag{7}$$

$$f^{lh\to e}_{\nu,\nu'}(u) = \lambda_1 - 2(\sqrt{1/4 + (2E^{e}_{\nu}(a,c)/(2E_g))}), \tag{8}$$

where $\mu_e = \mu_{lh} = 0.15m_0$ and $\mu_h \equiv \mu_{hh} = 0.5m_0$ are the masses of electron, light and heavy holes, respectively, $\tilde{E}_g = 180$ meV is the band gap width, $\kappa = 16$ is the dc permittivity, and $E^e_R = E^{lh}_R = e^2/(2\kappa a^e_B) = 7.972$ meV, $a^e_B = a^{lh}_B = \hbar^2\kappa/(\mu_e e^2) = 56.44\mathring{A}$, $E^h_R = E^{hh}_R = e^2/(2\kappa a^{hh}_B) = 26.57$ meV, $a^h_B = a^{hh}_B = \hbar^2\kappa/(\mu_h e^2) = 16.93$Å.

For both electron and hole carriers the dimensionless energies $2E^e_\nu = \tilde{E}^e_\nu/\tilde{E}^e_R$ and $2E^h_\nu(\mu_h/\mu_e) = \tilde{E}^h_\nu/\tilde{E}^e_R$ are expressed in the same reduced atomic units $\tilde{E}^e_R$, and the overlap integral (2) between the eigenfunctions, corresponding to $E^e_\nu(\gamma_F)$ and $E^h_\nu(\gamma_F) = (\mu_e/\mu_h)E^e_\nu(-(\mu_h/\mu_e)\gamma_F)$, takes the form

$$\tilde{I}_{\nu,\nu'}(u) = \left| \int \Psi^e_\nu(\mathbf{r}; a, c, \gamma_F, \mu_e)\Psi^e_{\nu'}(\mathbf{r}; a, c, -(\mu_h/\mu_e)\gamma_F, \mu_e)d^3\mathbf{r} \right|^2. \tag{9}$$

Now consider an ensemble of OSQDs (or PSQDs), differing in the minor semiaxis values $c = u_o\bar{c}$ (or $a = u_p\bar{a}$), determined by the random parameter $u = u_o$ (or $u = u_p$). The corresponding minor semiaxis mean value is $\bar{c}$ at fixed major semiaxis a (or $\bar{a}$ at fixed major semiaxis c), and the appropriate distribution function is $P(u_o)$ (or $P(u_p)$). Commonly, in this case the normalized Lifshits-Slezov distribution function [17] is used:

$$P(u) = \{3^4 e u^2 \exp(-1/(1-2u/3))/2^{5/3}/(u+3)^{7/3}/(3/2-u)^{11/3}, u \in (0, 3/2); 0, \text{otherwise}\}$$

having conventional properties $\int P(u)du = 1$, $\bar{u} = \int uP(u)du = 1$. The absorption coefficients $\tilde{K}^o(\tilde{\omega}^{ph}, \bar{\tilde{a}}, \tilde{c})$ or $\tilde{K}^p(\tilde{\omega}^{ph}, \tilde{a}, \bar{\tilde{c}})$ of an ensemble of semiconductor OSQDs or PSQDs with different dimensions of minor semiaxes are expressed as

$$\tilde{K}^o(\tilde{\omega}^{ph}, \bar{\tilde{a}}, \tilde{c}) = \int \tilde{K}(\tilde{\omega}^{ph}, \bar{\tilde{a}}, \tilde{c}, u_o)P(u_o)du_o, \quad \tilde{K}^p(\tilde{\omega}^{ph}, \tilde{a}, \bar{\tilde{c}}) = \int \tilde{K}(\tilde{\omega}^{ph}, \tilde{a}, \bar{\tilde{c}}, u_p)P(u_p)du_p. \tag{10}$$

Substituting (3) into (10) and taking into account the known properties of the δ-function, we arrive at the analytical expression for the absorption coefficient $\tilde{K}(\tilde{\omega}^{ph}, \tilde{a}, \tilde{c})$ of a system of semiconductor QDs with a distribution of random minor semiaxes:

$$\frac{\tilde{K}(\tilde{\omega}^{ph})}{\tilde{K}_0} = \sum_{\nu,\nu',s} \frac{\tilde{K}_{\nu,\nu'}(\tilde{\omega}^{ph})}{\tilde{K}_0}, \quad \frac{\tilde{K}_{\nu,\nu'}(\tilde{\omega}^{ph})}{\tilde{K}_0} = \tilde{I}_{\nu,\nu'}(u_s) \left| \frac{df_{\nu,\nu'}(u)}{du} \right|_{u=u_s} \Bigg|^{-1} P(u_s), \tag{11}$$

where $\tilde{K}_0 = \tilde{A}^{-1}\tilde{E}_g$ is the normalization factor, u_s are the roots of the equation $f_{\nu,\nu'}(u_s) = 0$.

At $\gamma_F = 0$ for IPBM we have the interband overlap $\tilde{I}_{\nu,\nu'} = \delta_{n_{\rho o},n'_{\rho o}}\delta_{n_{zo},n'_{zo}}\delta_{m,-m'}$ for OSQD, or $\tilde{I}_{\nu,\nu'} = (J_{1+|m|}(\alpha_{n_{\rho p}+1,|m|})/J_{1-|m|}(\alpha_{n_{\rho p}+1,|m|}))^2\delta_{n_{zp},n'_{zp}}\delta_{n_{\rho p},n'_{\rho p}}\delta_{m,-m'}$ for PSQD, where $\alpha_{n_{\rho p}+1,|m|}$ is the positive root of the Bessel function, and the selection rules $m = -m'$, $n_{zo} = n'_{zo}$, $n_{\rho o} = n'_{\rho o}$, or $n_{\rho p} = n'_{\rho p}$, $n_{zp} = n'_{zp}$ [31], while at $\gamma_F \neq 0$ one should calculate the interband overlap (9) in accordance with the selection rules $m = -m'$, $n_{\rho o} = n'_{\rho o}$, or $n_{\rho p} = n'_{\rho p}$ [41], respectively. Note that the contributions of non-diagonal matrix elements to the energy values are about 1% for IPBM of OSQD and PSQD; then in the Born-Oppenheimer approximation of the order b_{max} for the AC we get [31, 41]

$$f_{\nu,\nu'}(u) = \lambda_1 - \sum_{j=0}^{b_{max}} \check{E}^{(j)} u^{j-2}. \tag{12}$$

For example, at $\gamma_F = 0$ the coefficients $\check{E}^{(j)}$ are defined by [31]

$$\begin{aligned}
&\check{E}^{(j)} = (2E_g)^{-1}E^{(j)}_{io}\omega^{2-j}_{\rho;n_o}(\bar{c})(1+\mu_e/\mu_h) \quad \text{or} \quad \check{E}^{(j)} = (2E_g)^{-1}E^{(j)}_{ip}\omega^{2-j}_{z;n_{\rho p}}(\bar{a})(1+\mu_e/\mu_h),\\
&\omega_{\rho;n_o}(\bar{c}) = \pi n_o/(a\bar{c}), \quad \omega_{z;n_{\rho p}}(\bar{a}) = \alpha_{n_{\rho p}+1,|m|}/(\bar{a}c);\\
&E^{(0)}_{io} = a^2/4, \quad E^{(1)}_{io} = (2n_{\rho o}+|m|+1), \quad E^{(2)}_{io} = (6n_{\rho o}|m|+2+6n_{\rho o}+6n^2_{\rho o}+|m|^2+3|m|)a^{-2},\\
&E^{(3)}_{io} = 3(6n_{\rho o}+3|m|+2+|m|^2+6n^2_{\rho o}+6n_{\rho o}|m|+4n^3_{\rho o}+6|m|n^2_{\rho o}+2|m|^2n_{\rho o})a^{-4}/2;\\
&E^{(0)}_{ip} = c^2, \quad E^{(1)}_{ip} = (2n_{zp}+1), \quad E^{(2)}_{ip} = +3(2n_{zp}+2n^2_{zp}+1)c^{-2}/4,\\
&E^{(3)}_{ip} = 3(3n^2_{zp}+7n_{zp}+2n^3_{zp}+3)c^{-4}/16.
\end{aligned} \tag{13}$$

For the Lifshits-Slezov distribution Figs. 2 and 3 display the total absorption coefficients $\tilde{K}(\tilde{\omega}^{ph})/\tilde{K}_0$ and the partial absorption coefficients $\tilde{K}_{\nu,\nu}(\tilde{\omega}^{ph})/\tilde{K}_0$, that form the corresponding partial sum (11) over a fixed set of quantum numbers ν, ν' at $m = -m' = 0$. As a result of averaging (10) a series of curves with finite with and height are observed instead of a series of δ-functions. One can see that, in the first place, the summation over the quantum numbers $n_o = n_{zo}+1 = 1, 2, 3, 4, 5$ (or $n_p = n_{\rho p}+1 = 1, 2, 3$) enumerating the nodes of the wave function with respect to the fast variable gives the corresponding principal maxima of the total AC for the ensemble of QDs with distributed dimensions of minor semiaxis. Secondly, the summation over the quantum number $n_{\rho o} = 0, 1, 2, 3, ..., 8$ (or $n_{zp} = 0, 1, 2, ..., 15$) that labels the nodes of the wave function with respect to the slow variable leads to the increase of amplitudes of these maxima and to secondary maxima arising in the case of sparer energy levels of IPBM of OSQDs (or PSQDs).

In the regime of strong dimensional quantization the frequencies $\Delta\tilde{\omega}^{ph}_{100}/(2\pi) = (2\pi\hbar)^{-1}(\tilde{W}_{100,100} - \tilde{E}_g)$ of the interband transitions ($h \to e$) in GaAS between the levels $n_o = 1, n_{\rho o} = 0, m = 0$ for OSQD or $n_p = 1, n_{zp} = 0, m = 0$ for PSQD at the fixed values $\tilde{a} = 2.5a_e$ and $\tilde{c} = 0.5a_e$ for OSQD or $\tilde{a} = 0.5a_e$ and $\tilde{c} = 2.5a_e$ for PSQD, are equal to $\Delta\tilde{\omega}^{ph}_{100}/(2\pi) = 16.9$THz at $\gamma_F = 0$ and $\Delta\tilde{\omega}^{ph}_{100}/(2\pi) = 15.9$THz at $\gamma_F = 10$, or $\Delta\tilde{\omega}^{ph}_{100}/(2\pi) = 33.3$THz at $\gamma_F = 0$ and $\Delta\tilde{\omega}^{ph}_{100}/(2\pi) = 31.5$THz at $\gamma_F = 2$ correspond to the infra-red spectral region [9, 10], taking the band gap value $(2\pi\hbar)^{-1}\tilde{E}_g = 346$THz into account. In Fig. 3 one can see the quantum-confined Stark effect that consist in the reduction of the absorption energy (light frequency) at the expense of lowering the energy of both (e) and (h) bound states due to the electric field effect. The total ACs at $F \neq 0$, shown by solid lines, qualitatively correspond to the total AC at $F = 0$, shown by dashed lines, but have lower magnitudes and smooth behavior, in spite of the additional contribution to the partial ACs of

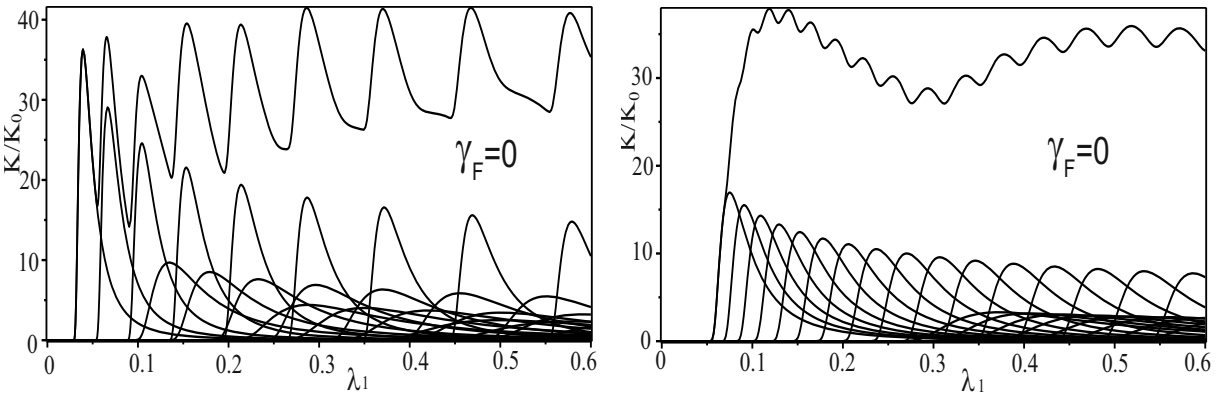

Figure 2. Absorption coefficient K/K_0, Eq. (11), consisting of a sum of the first partial contributions vs the energy $\lambda = \lambda_1$ of the optical interband transitions for the Lifshits-Slezov distribution, using the functions $f^{h\to e}_{\nu,\nu'}(u)$ for GaAs ($h \to e$) without electric field: for ensemble of OSQDs $\bar{c} = 0.5$, $a = 2.5$ (left panel) and for ensemble of PSQDs $\bar{a} = 0.5$, $c = 2.5$ (right panel).

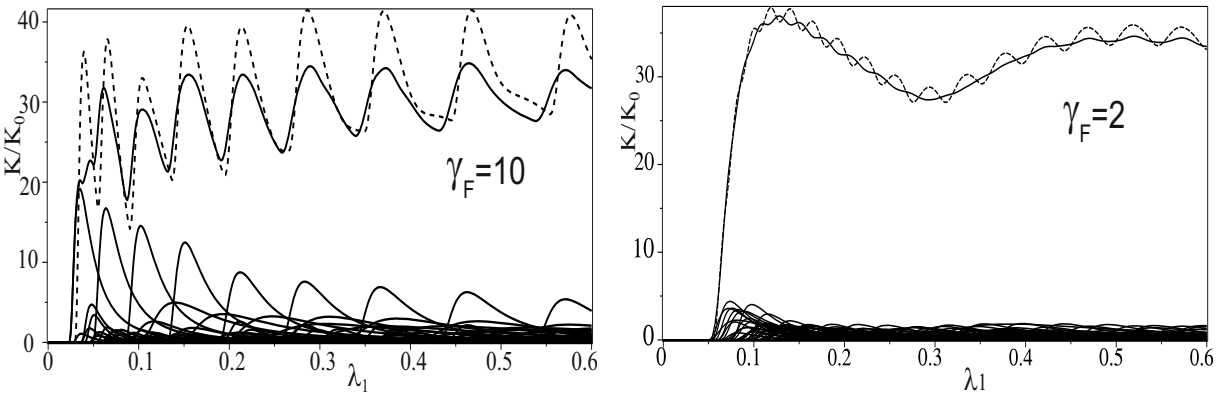

Figure 3. The same as in Fig. 2, but in the presence of electric field $2\gamma_F = F/F_0^*$. For comparison, the corresponding absorption coefficient without electric field is given by dashed line.

the overlap integral (9) from the interband transition $n_{zo} \neq n'_{zo}$ or $n_{zp} \neq n'_{zp}$ in OSQD or PSQD, also shown in Fig. 3.

At the same parameters of the QDs the frequencies of the interband transitions ($lh \to e$) in InSb are equal to $\Delta\tilde{\omega}^{ph}_{100}/(2\pi) = 68.5$THz for OSQD or $\Delta\tilde{\omega}^{ph}_{100}/(2\pi) = 87.2$THz for PSQD, while the frequencies of the interband transitions ($hh \to e$) in InSb are equal to $\Delta\tilde{\omega}^{ph}_{100}/(2\pi) = 78.6$THz for OSQD or $\Delta\tilde{\omega}^{ph}_{100}/(2\pi) = 102$THz for PSQD. These values correspond to the infrared spectral region with longer wavelength, similar to [24], with the band gap value $(2\pi\hbar)^{-1}\tilde{E}_g = 44$THz taken into account. One can see that the behavior of total ACs for parabolic dispersion law for IPBM of InSb, shown in Fig. 4, is similar to that for GaAs (Fig. 2), while the behavior of AC for nonparabolic dispersion law, shown in Fig. 5, is essentially different. In particular, for OSQDs it grows faster with increasing λ_1, while for PSQDs it goes to a plateau before starting to grow. Indeed, with increasing quantum numbers $n_{\rho o}$ or n_{zp} that characterize the excitation of slow motion, the maxima of partial ACs decrease for parabolic dispersion law, while for the nonparabolic one the maxima of partial ACs increase.

With decreasing semiaxis the threshold energy increases, because the "effective" band gap

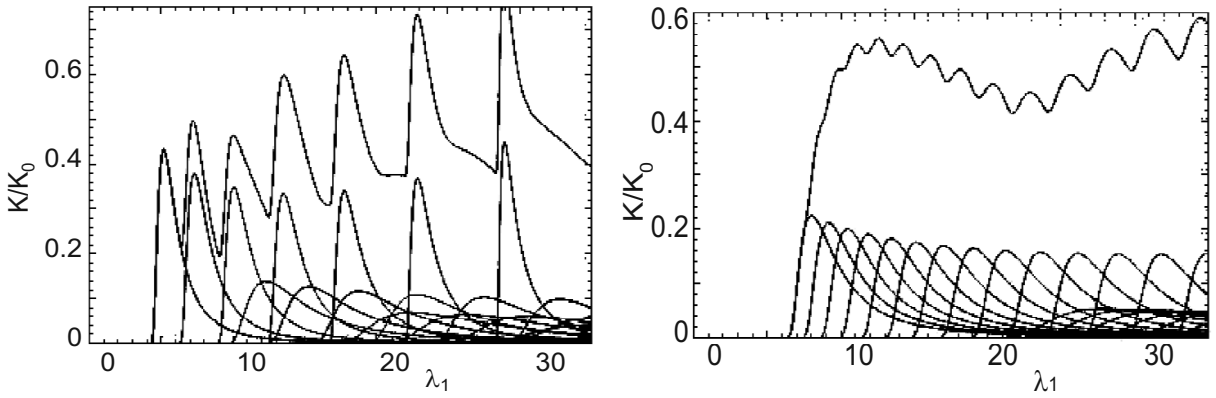

Figure 4. The same as in Fig. 2, but for InSb ($hh \to e$) interband transition.

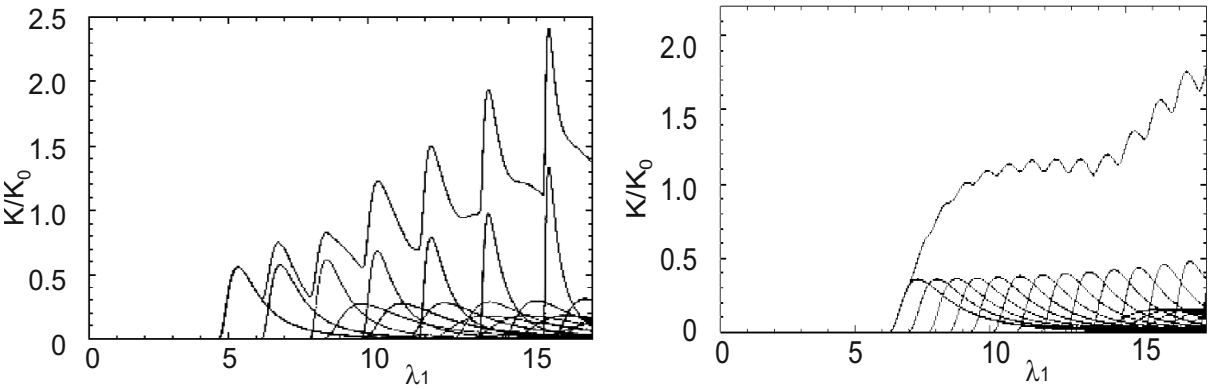

Figure 5. The same as in Fig. 2, but for InSb ($lh \to e$) interband transition.

width increases, which is a consequence of the dimensional quantization enhancement. Therefore, the above frequency is greater for PSQD than for OSQD, because the SQ implemented in two direction of the plane (x,y) is effectively larger than that in the direction of the z axis solely at similar values of semiaxes. Higher-accuracy calculations reveal an essential difference in the frequency behavior of the AC for interband transitions in systems of semiconductor OSQDs or PSQDs having a distribution of minor semiaxes, which can be used to verify the above models.

4. Conclusion

In this paper we demonstrate the efficient methods of calculating the electron and hole states in the presence of an electric field for spherical and spheroidal QDs with parabolic and non-parabolic dispersion laws. Our analysis shows that the adiabatic approach provides a useful theoretical tool for describing absorption coefficients in an ensemble of spheroidal QDs with random distribution of minor semiaxes. Further development and applications of our approach and SNAs are associated with the investigation of exciton effects, as well as electron-electron and hole-hole interactions in spheroidal QDs.

The work was supported partially by RFBR (grants No 10-02-00200 and 11-01-00523).

[1] Bimberg D, Grundman M, Ledentsov N 1999 *Quantum Dot Heterostructures* (Wiley, New-York)
[2] Alferov Zh 1998 *Semiconductors* **32** 1
[3] Li Bin et al 2007 *Phys. Lett. A* **367** 493
[4] Lamouche G, Lépine Y 1994 *Phys. Rev. B* **49** 13452
[5] Hawrylak P, Wojs A 1996 *Semicond. Sci. Technol.* **11** 1516

[6] Sarkisyan H A 2002 *Mod. Phys. Lett. B* **16** 835
[7] Dvoyan K G et al 2012 *Int. J. Mod. Phys. Conf. Ser.* **15** 40
[8] Nazmitdinov R G 2009 *Phys. Part. Nucl.* **40** 71
[9] Dvoyan K G et al 2009 *Nanoscale Res. Lett.* **4** 106; Dvoyan K G et al 2010 *Proc. SPIE* **7998** 79981F
[10] Dvoyan K G et al 2007 *Nanoscale Res. Lett.* **2** 601
[11] López S et al 2008 *Physica E* **40** 1383
[12] Barseghyan M, Kirakosyan A, Duque C 2009 *Eur. Phys. J. B* **72** 521
[13] Gharaati A, Khordad R 2010 *Superlattices Microstruct* **48** 276
[14] Filikhin I, Suslov V M, Vlahovic B 2006 *Phys. Rev. B* **73** 205332
[15] Filikhin I el al, 2009 *Physica E* **41** 1358
[16] Efros Al L, Efros A L 1982 *Sov. Phys. Semicond.* **16** 772
[17] Lifshits I M and Slezov V V 1958 *Sov. Phys. JETF.* **35** 479
[18] Moiseev K et al 2007 *Tech. Phys. Lett.* **33** 295
[19] Moiseev K et al 2009 *Semiconductors* **43** 1102
[20] Kane E O 1957 *J. Phys. Chem. Sol.* **1** 249
[21] Askerov B 1985 *Electronic Transport Phenomena in Semiconductors* (Nauka, Moscow)(in Russian)
[22] Kazaryan E, Meliksetyan A, Sarkisyan H 2007 *Tech. Phys. Lett.* **33** 964
[23] Kazaryan E, Meliksetyan A, Sarkisyan H 2010 *J. Comput. Theor. Nanosci.* **7** 486
[24] Atoyan M S et al 2011 *Physica E* **43** 1592
[25] Cantele G et al, 2000 *J. Phys.: Cond. Matt.* **12,** 9019
[26] Van den Broek M and Peeters F M, 2001 *Physica E* **11,** 345.
[27] Trani F et al, 2005 *Phys. Rev. B* **72,** 075423
[28] Lepadatu A-M et al, 2010 *J. Appl. Phys.* **107,** 033721
[29] Bagga A, Ghosh S, and Chattopadhyay P K 2005 *Nanotechnology* **16** 2726
[30] Gusev A A et al 2010 *Lect. Notes Comp. Sci.* **6244** 106
[31] Gusev A A et al 2012 *Phys. Atom. Nucl.* **75** 1210
[32] Gusev A A et al 2010 *J. Phys. Conf. Ser.* **248** 012047
[33] Gusev A A et al 2010 *Phys. Atom. Nucl.* **73** 352
[34] Chuluunbaatar O et al 2007 *Comput. Phys. Commun.* **177** 649
[35] Chuluunbaatar O et al 2009 *Comput. Phys. Commun.* **180** 1358
[36] Chuluunbaatar O et al 2008 *Comput. Phys. Commun.* **179** 685
[37] Gerdt V et al 2006 *Lect. Notes Comp. Sci.* **4194** 194
[38] Chuluunbaatar O et al 2008 *Comput. Phys. Commun.* **178** 301
[39] Chuluunbaatar O et al 2007 *Lect. Notes Comp. Sci.* **4770** 118
[40] Gusev A A et al 2012 *Lect. Notes Comp. Sci.* **7442** 155
[41] Gusev A A et al 2013 *Phys. Atom. Nucl.* **76** submitted
[42] Kazaryan E M, Petrosyan L S, Sarkisyan H A 2003 *Physica E* **16** 174
[43] Zoheir M, Manaselyan A Kh, Sarkisyan H A 2008 *Physica E* **40** 2945